

CO₂ Laser Glazing Treatment of a Veneering Porcelain: Effects on Porosity, Translucency, and Mechanical Properties

R Sgura • MC dos Reis • MC Salvadori
AC Hernandez • PF Cesar • IS Medeiros

Clinical Relevance

Since laser glazing is a fast and viable procedure it could be considered for chairside application in ceramic restorations, reducing the number of appointments required in the dental office.

SUMMARY

This work tested CO₂ laser as a glazing agent and investigated the effects of irradiation on the porosity, translucency, and mechanical properties of veneering porcelain. Sixty discs

*Ricardo Sgura, University of Sao Paulo, Department of Biomaterials and Oral Biology, Sao Paulo, Brazil

Mariana Cavalcante dos Reis, University of Sao Paulo, Department of Biomaterials and Oral Biology, Sao Paulo, Brazil

Maria Cecília Salvadori, University of Sao Paulo, Institute of Physics, Sao Paulo, Brazil

Antônio Carlos Hernandez, University of Sao Paulo, Sao Carlos Institute of Physics, Sao Paulo, Brazil

Paulo Francisco Cesar, University of Sao Paulo, Department of Biomaterials and Oral Biology, Sao Paulo, Brazil

Igor Studart Medeiros, Sao Paulo, Brazil

*Corresponding author: Av. Professor Lineu Prestes, 2227 – Cidade Universitária. Departamento de Biomateriais e Biologia Oral, Faculdade de Odontologia. São Paulo, SP, 05508000, Brasil; e-mail: risgura@hotmail.com

DOI: 10.2341/14-079-L

(diameter 3.5 × 2.0 mm) of veneering porcelain for Y-TZP frameworks (VM9, VITA Zahnfabrik) were sintered and had one of their faces mirror polished. The specimens were divided into six groups (n=10/group) according to surface treatment, as follows: no treatment-control; auto-glaze in furnace following manufacturer's instructions (G); and CO₂ laser (45 or 50 W/cm²) applied for four or five minutes (L45/4, L45/5, L50/4, L50/5). Optical microscopy (Shimadzu, 100×) was conducted and the images were analyzed with Image J software for the determination of the following porosity parameters: area fraction, average size, and Feret diameter. The translucency parameter studied was masking ability, determined by color difference (ΔE) over black and white backgrounds (CM3370d, Konica Minolta). Microhardness and fracture toughness (indentation fracture) were measured with a Vickers indenter (HMV, Shimadzu). Contact atomic force microscopy (AFM) (50 × 50 μm², Nanoscope IIIA, Veeco) was performed at the center of one sample from

each group, except in the case of L45/5. With regard to porosity and translucency parameters, auto-glazed and laser-irradiated specimens presented statistical similarity. The area fraction of the surface pores ranged between 2.4% and 5.4% for irradiated specimens. Group L50/5 presented higher microhardness when compared to the G group. The higher (1.1) and lower (0.8) values for fracture toughness ($\text{MPa}\cdot\text{m}^{1/2}$) were found in laser-irradiated groups (L50/4 and L45/4, respectively). AFM performed after laser treatment revealed changes in porcelain surface profile at a sub-micrometric scale, with the presence of elongated peaks and deep valleys.

INTRODUCTION

Glazing is a fundamental step during the production of dental ceramic restorations, which consists of an application of a transparent, viscous, and low-fusion ceramic frit on the porcelain surface in order to increase smoothness and gloss after a new firing cycle (glazing cycle).¹⁻⁴ One variation of this type of glaze procedure is the so-called "auto-glaze," which involves an additional firing cycle without the addition of an external ceramic layer to the porcelain piece.⁵ The auto-glaze cycle is carried out at low temperatures aiming at softening the outermost superficial layer of the ceramic restoration without changing its shape. Both glazing methods described above decrease the number of surface flaws^{6,7} and create surface compressive stresses, increasing the lifetime of the ceramic structure.⁸⁻¹⁰

The reduction and elimination of surface defects is one of the most advantageous aspects of any glazing technique, since surface flaws and pores may act as stress concentrators and lead to the catastrophic failure of the material in the long term.^{5,11-14} External surface flaws usually appear during the processing of the prostheses or after intraoral occlusal/interproximal adjustments.^{12,15} Pores are different types of flaws that occur in dental porcelains as a consequence of viscous flow sintering. They may also appear in the glassy matrix of a porcelain as a result of bubble formation after the release of dissolved or entrapped insoluble gases that are present in the initial pores.¹⁶

In addition to the negative effect of surface flaws and pores on the porcelain mechanical strength, they also jeopardize the optical properties of the material. Surface irregularities such as grooves and cracks increase light scattering at the surface and therefore make the material more opaque.¹⁷ Residual pores

also affect light transmission, as they act as scattering centers within the material. When light propagates within a material and reaches a pore, it deviates from its normal path as a result of the difference in refraction index between the pore medium (air) and the porcelain material.¹⁸

Alternative glazing treatments have been suggested in the literature (eg, microwave oven¹⁹ and CO_2 laser sintering²⁰), with promising results. Continuous CO_2 laser irradiation of ground porcelain discs resulted in surface roughness similar to that of auto-glazed specimens. In the same study, the color difference (ΔE) between irradiated and glazed specimens was not considered perceivable to the human eye for most experimental groups. The advantages of CO_2 laser glazing are 1) the possibility of reducing the number of appointments that they offer, since laser application is a chairside technique, and 2) the higher processing speed, which is approximately four times faster than that of the conventional technique.²⁰

To the authors' knowledge, the effects of CO_2 laser glazing on porosity and translucency have not yet been determined. Therefore, this study evaluated the surface porosity, masking ability, microhardness, and apparent fracture toughness of a commercial veneering porcelain submitted to CO_2 laser glazing. The surface profiles of irradiated specimens were also assessed by atomic force microscopy (AFM). The hypothesis tested was that, for the characterizations cited above, CO_2 laser glazing would be similar to auto-glazing in a conventional furnace.

METHODS AND MATERIALS

The porcelain used in this study was VM9 (VITA-Zahnfabrik, Bad Sackingen, Germany), which is recommended to veneer Y-TZP substrates. Sixty porcelain discs were produced using a metallic device in order to standardize their dimensions to 4.1×2.4 mm (diameter \times thickness). These discs were then sintered (Kerampress, Kota, São Paulo, SP, Brazil) following the heating cycle recommended by the manufacturer (Table 1). The final dimensions of the specimens after sintering were 3.5×2.0 mm. Specimens had one of their faces ground and polished with diamond abrasive suspensions ranging from 15 to 1 μm (Ecomet 3, Buehler, Lake Buff, IL, USA).

Specimens were then divided into 10 groups according to the surface treatment (Table 2). For group G, specimens were submitted to the glaze cycle

Table 1: Sintering and Glazing Furnace Cycles Applied to VM9 Porcelain

	Sintering Cycle	Glaze Cycle
Dry, min	6	4
Start temperature, °C	500	500
Heating rate, °C/min	55	80
Maximum temperature, °C	910	900
Vacuum shutdown, °C	910	No vacuum
Sintering time, min	1.5	2
Cooling time, min	6	6

described in Table 1 in a conventional furnace. A 10.6- μm CO₂ laser device (35 W, Coherent, Santa Clara, CA, USA) was used for the surface treatment of specimens in groups L45 and L50. A copper mirror was used to focus the laser beam onto a refractory with a spot size of 0.5 cm, and the distance between the laser tip and the porcelain disc was kept constant during the experiment, as illustrated in Figure 1. The laser outputs tested were 9 and 10 W, which corresponded to the irradiances of 45 and 50 W/cm². The laser beam was continuously irradiated for four or five minutes, according to each group. Irradiance and time were chosen based on a previous study.²⁰

For surface porosity determination, three images per specimen were obtained at 100 \times magnification (HMV, Shimadzu, Singapore). Micrographs were analyzed with Image J software (National Institutes of Health, Bethesda, MD, USA) for determination of the area fraction and Feret diameter of pores. Mean values were submitted to Kruskal-Wallis one-way analysis of variance (ANOVA) ($p=0.05$). The Feret diameter was also used to determine the pore size at the 90% cumulative frequency (D90).

Microhardness and apparent fracture toughness (indentation fracture, IF) were determined by measuring the cracks produced on the specimen surface by a Vickers indenter (HMV, Shimadzu).

For microhardness determination (measured in GPa) the following formula was applied:

$$\left(1.8544 \frac{F}{d^2}\right) 0.009807,$$

where F is the applied load in Kgf, and

$$d = \frac{d_h + d_v}{2},$$

where d_h and d_v are the horizontal and vertical indentation diagonals, respectively.

The formula proposed by Lawn and others²¹ was used to determine the apparent fracture toughness, as follows:

$$K_{IC} = 0.028 \left(\frac{E}{H}\right)^{1/2} H d^{1/2} \left(\frac{c}{d}\right)^{-3/2},$$

where E is the elastic modulus of VM9 porcelain (66.5), c is the crack length observed after indentation, and H is the Vickers microhardness, in GPa.

Indentations were produced with a load of 2.0 Kgf, and the dwell time was 20 seconds. Three indentations were made per specimen, and mean values were compared by ANOVA and Tukey test, with global significance level of 5%.

To determine the effect of laser application on the material's ability to mask a dark substrate, the color difference (ΔE) between specimens positioned over a black or white substrate was calculated with a spectrophotometer (CM-3700d, Konica Minolta, Sakai, Osaka, JP), according to the following equation:

$$\Delta E = \left[(L_B - L_w)^2 + (a_B - a_w)^2 + (b_B - b_w)^2 \right]^{1/2},$$

where L , a , and b parameters refer to the color coordinates of lightness, degree of redness/greenness, and degree of yellowness/blueness, respectively, as designated by the Commission International de l'Eclairage.²² Subscripts B and W represent the black and white backgrounds, respectively.

Black and white standardized cards were used to simulate the substrates. A coupling agent (glycerin)

Table 2: Groups Distribution ($n=10$)

Group	Fluence, J/cm ²	Surface Treatment	Designation	
Control	—	Polishing	C	
Auto-glaze	—	Polishing + glaze in furnace	G	
Laser 45 W/cm ²	4 min	10,800	Polishing + continuous CO ₂ laser	L45/4
	5 min	13,500	Polishing + continuous CO ₂ laser	L45/5
Laser 50 W/cm ²	4 min	12,000	Polishing + continuous CO ₂ laser	L50/4
	5 min	15,000	polishing + continuous CO ₂ laser	L50/5

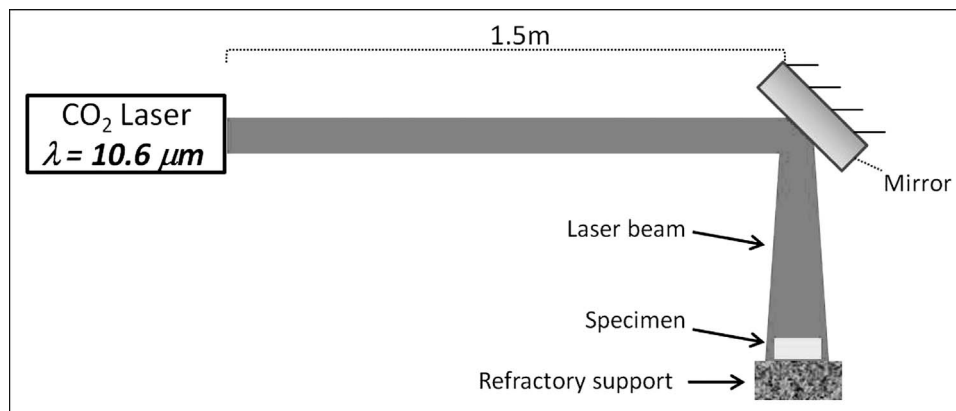


Figure 1. Optical table disposal for laser irradiation. Laser was continuously irradiated over sintered specimens (0.5-cm spot size).

with same refractive index of the studied porcelain was applied between the porcelain disc and the background. The means of masking ability were submitted to ANOVA and a Tukey *post hoc* test, with global significance level of 5%. The surface profile of one specimen from each of the following groups—L45/4, L50/4, and L50/5—was assessed by AFM and compared to the profiles obtained for groups C and G. Contact AFM (Nanoscope IIIA, Veeco, Plainview, NY, USA) analysis was conducted using a scanned area of $50 \times 50 \mu\text{m}^2$ located at the center of the specimen surface. The AFM resolution was 512 pixels. Three-dimensional image processing was carried out with WSxM 5.0 software (Nanotech, Madrid, Spain).²³

RESULTS

The porosity parameters are described in Table 3. The total area fraction of pores increased significantly after treating the specimens with almost all laser glazing procedures. The only exception was the surface treatment involving the combination of a laser irradiance of 50 W/cm^2 and an application time of five minutes, which resulted in porosity similar to that of the control group. The means of pore sizes, as expressed by the Feret diameter, were similar for all experimental groups and varied from 7.1 to $8.5 \mu\text{m}$. The parameter D90 increased, in comparison to the

control, from 32% to 52% for the different glazing treatments.

The optical micrographs in Figure 2 show the heterogeneous distribution of the pores described in Table 3. One important aspect that should be highlighted in Figure 2 is the presence of striations on the surface of the specimens glazed at 50 W/cm^2 for five minutes. These striations could also be noticed on the surface of specimens from groups L45/5 and L50/4; however, they were not as clear and numerous as on the surface of the specimens in group L50/5.

Figure 3 shows that the use of laser irradiation as a glazing treatment for the studied porcelain resulted in a significant increase in microhardness in comparison to the auto-glazed group only for the group treated at 50 W/cm^2 for five minutes. The fracture toughness values depicted in Figure 3 varied significantly as a function of the experimental group. The K_{Ic} values obtained for two of the laser-treated groups (L45/5 and L50/5) were similar to that obtained for the auto-glaze group. The other two laser-irradiated groups, L45/4 and L50/4, showed, respectively, lower and higher mean fracture toughness mean values in comparison to the auto-glaze group.

The means of translucency parameter (masking ability, ΔE) obtained for specimens submitted to CO₂

Table 3: Means and Standard Deviations (in Parentheses) for Porosity. D90 Corresponds to the Feret Diameter of Pores at 90% of Cumulative Frequency. Mean Values of Area Fraction Exhibiting the Same Letters Were Not Significantly Different ($p > 0.05$). There Were Not Statistical Differences Among the Mean Values of Feret Diameter ($p = 0.58$)

Groups	C	G	L45/4	L45/5	L50/4	L50/5
Area fraction, %	1.2 (0.9) A	3.6 (1.4) BC	4.3 (1.2) BC	5.4 (1.4) C	4.4 (2.4) C	2.4 (1.0) AB
Feret diameter, μm	7.4 (2.1)	7.3 (1.1)	7.8 (2.6)	7.8 (1.1)	7.1 (1.3)	8.5 (2.0)
D90, μm	11.4	16.9	16.0	18.4	15.0	17.0

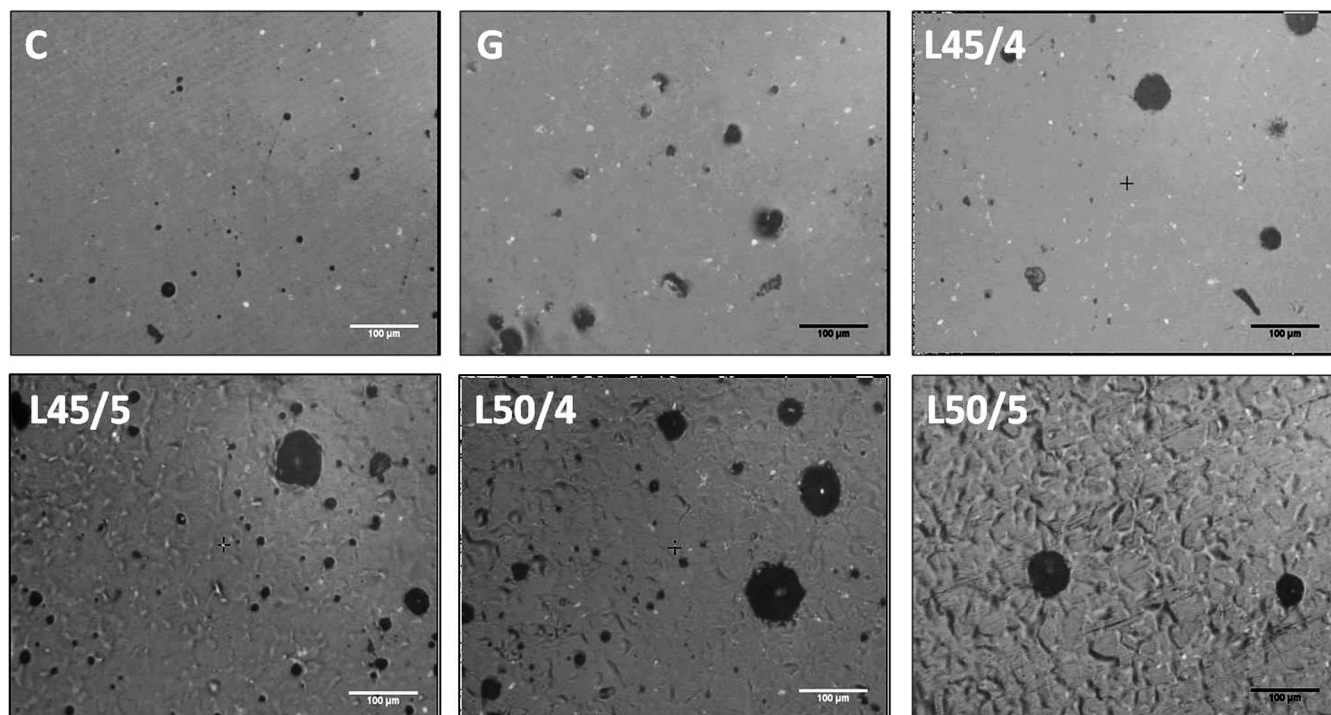


Figure 2. Optical microscopy images (100 \times) of studied groups. In figure L50/5 it is possible to observe the striations formation.

laser were statistically similar to that found for group G. Group L45/5 showed the lowest ΔE value among all groups; however, it was only statistically different from the mean obtained for the control (Figure 3C).

Surface profiles assessed by AFM showed sub-micrometric surface modifications on the porcelain specimens after laser irradiation. All laser-irradiated surfaces showed elongated, rounded peaks and deep valleys (Figure 4). The surface of the control was flat and showed grooves resulting from the polishing procedure. These polishing grooves were also noticeable on the surface of groups G and L45/4; however, their depth was significantly lower (arrows in Figure 4). Polishing grooves were not found in images from groups L50/4 and L50/5.

DISCUSSION

The hypothesis that CO₂ laser glazing would be similar to auto-glazing in a conventional furnace could only be partially accepted, because although these two surface treatments resulted in similar porosity and translucency, some of the laser parameters tested resulted in significantly different microhardness, apparent fracture toughness, and surface topography.

Although it was expected that the energy provided by the glazing treatments would favor viscous flow

and therefore reduce surface porosity, the results indicated that in fact a significantly higher number of pores was found after all types of glazing. Such an increase in porosity observed for most glazed groups in comparison to the control may be related to the displacement of subsurface pores toward the surface as a result of the decrease in the porcelain's viscosity at high temperatures.¹⁶ The observed increase in pore size after heat treatment (see D90 values in Table 3) suggests that moving pores are probably growing together as a consequence of energy increase during the glaze cycle.

The similar masking ability obtained for laser-glazed and oven-glazed specimens is likely directly related to the similar level of porosity found for these groups. It is well known that pores act as scattering centers that reduce the translucency of the material and therefore increase their ability to mask dark backgrounds.¹⁷ Not surprisingly, the group that showed the highest masking ability (lowest ΔE , L45/5) was also the one with the highest porosity.

The observed increase in microhardness for irradiated specimens may be explained by the increase in leucite content and size after continuous CO₂ laser irradiation, as described in a previous study.²⁰ On the other hand, the differences observed among the mean values of fracture toughness did not follow any

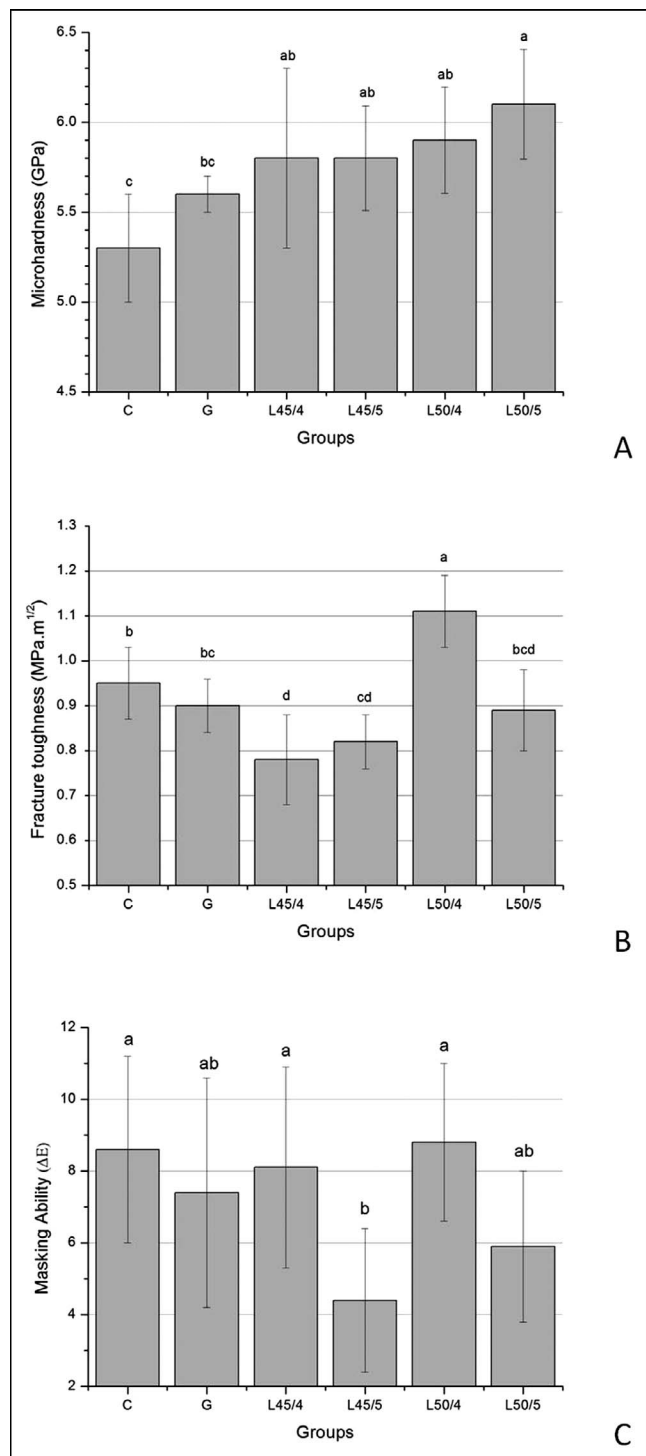


Figure 3. Graphical representation of microhardness (A), apparent fracture toughness (B), and masking ability (C) means with standard deviations. Means with different letters are significantly different ($p < 0.05$).

logical trend. It is believed that the different heat treatments applied to the porcelain surface resulted in significantly different distributions of residual stresses, which affected the crack growth that originated from the corner of the Vickers indentations during the IF test. Further studies are necessary to determine the level and distribution of residual stresses as a function of the glaze treatment performed.

AFM proved to be a fundamental tool with which to analyze the surface profile of irradiated specimens. Although a previous study²⁰ showed that laser-irradiated and oven-glazed porcelain had similar surface roughness when measured with a contact profilometer, the AFM analysis carried out in the present investigation showed important differences at the submicrometric scale (Figure 4). The better performance of AFM in comparison to a stylus profilometer has already been shown in a previous work,²⁴ in which subtle changes caused by conventional glazing on the porcelain surface could only be detected by the first method.

The round and elongated peaks observed at the center of the irradiated specimens (AFM analysis, Figure 4) and the lack of polishing grooves for groups L50/4 and L50/5 suggest that the temperature generated by the laser treatment led to melting of the outermost porcelain layer. To the authors' knowledge, these surface features observed after laser treatment in porcelain specimens under AFM have not been demonstrated before. The above-mentioned submicrometric peaks correspond to the striations observed under optical microscopy (Figure 2). The mechanism by which these striations are formed is not yet clear, but one possible explanation would be fluctuations in the distribution of the beam intensity, which can generate thermal gradients, as explained in a previous work²⁵ for a similar type of striation reported for ceramic pieces after CO₂ laser cutting.

The results of this study indicate that continuous CO₂ laser applied for four minutes with 50 W/cm² of irradiance over VM9 porcelain is able to produce a surface comparable to that achieved after an auto-glaze treatment with regard to surface porosity, masking ability, and microhardness, with an increase in the apparent fracture toughness. Further studies should take into account the submicrometric changes observed on the porcelain surface after laser incidence and how they would affect the tribological properties of porcelain pieces during functioning.

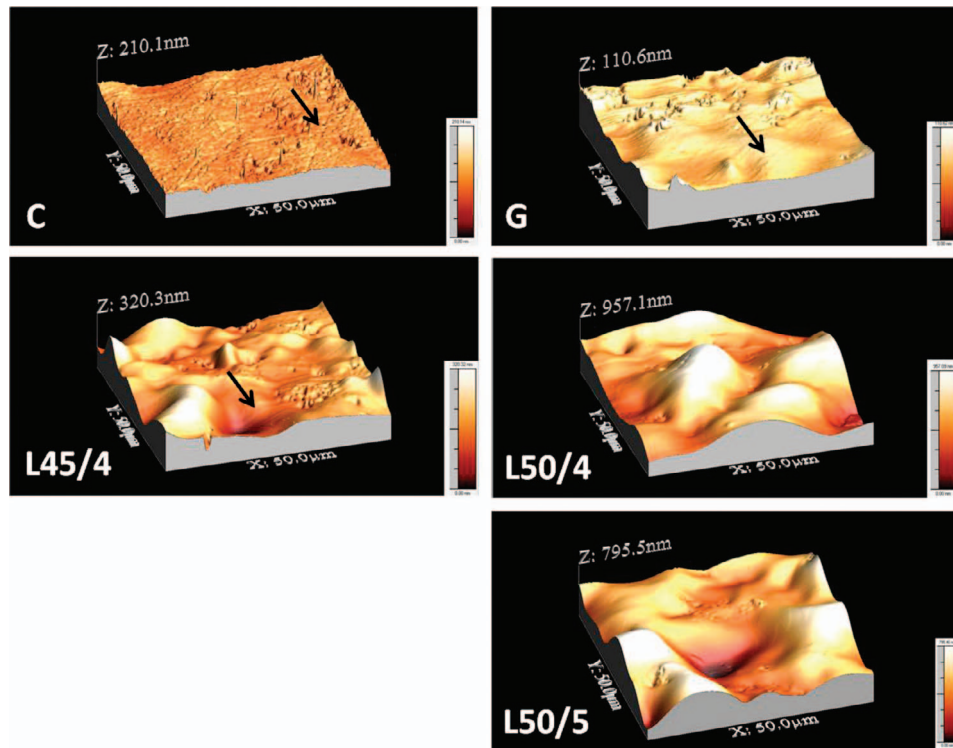


Figure 4. Atomic force microscopy. Arrow indicates grooves originated from polishing procedure. In groups L50/4 and L50/5 the grooves are not present. For all laser groups (L) it is possible to note the profile, characterized by rounded, elongated peaks and deep valleys.

CONCLUSIONS

The surface porosity and the masking ability observed in specimens submitted to laser treatment were similar to those of specimens auto-glazed in a furnace. Laser-glazed specimens presented a surface profile characterized by rounded and elongated peaks and deep valleys when assessed by AFM. At lower magnification, those surface changes resulted in striation formation, as observed by optical microscopy. With regard to mechanical properties, CO₂ laser glazing resulted in an increase in microhardness and changed the apparent fracture toughness of porcelain, depending on the irradiance/time tested.

Acknowledgements

The authors would like to thank Laboratório de Filmes Finos/ Institute of Physics – USP, São Paulo, for the AFM facilities and CAPES (Coordination for the Improvement of Higher Education Personnel) for their financial support.

Conflict of Interest

The authors of this manuscript certify that they have no proprietary, financial, or other personal interest of any nature or kind in any product, service, and/or company that is presented in this article.

(Accepted 27 May 2014)

REFERENCES

- Romero M, Rincon JM, & Acosta A (2002) Effect of iron oxide content on the crystallization of a diopside glass-ceramic glaze *Journal of the European Ceramic Society* **22(6)** 883-890.
- Raimondo RL Jr, Richardson JT, & Wiedner B (1990) Polished versus autoglazed dental porcelain *Journal of Prosthetic Dentistry* **64(5)** 553-557.
- Fuzzi M, Zaccheroni Z, & Vallania G (1996) Scanning electron microscopy and profilometer evaluation of glazed and polished dental porcelain *International Journal of Prosthodontics* **9(5)** 452-458.
- Barghi N, King CJ, & Draughn RA (1975) A study of porcelain surfaces as utilized in fixed prosthodontics *Journal of Prosthetic Dentistry* **34(3)** 314-319.
- Griggs JA, Thompson JY, & Anusavice KJ (1996) Effects of flaw size and auto-glaze treatment on porcelain strength *Journal of Dental Research* **75(6)** 1414-1417.
- Clayton JA, & Green E (1970) Roughness of pontic materials and dental plaque *Journal of Prosthetic Dentistry* **23(4)** 407-411.
- Podshadley AG, & Harrison JD (1966) Rat connective tissue response to pontic materials *Journal of Prosthetic Dentistry* **16(1)** 110-118.
- Williamson RT, Kovarik RE, & Mitchell RJ (1996) Effects of grinding, polishing, and overglazing on the flexure strength of a high-leucite feldspathic porcelain *International Journal of Prosthodontics* **9(1)** 30-37.

9. Chu FC, Frankel N, & Smales RJ (2000) Surface roughness and flexural strength of self-glazed, polished, and reglazed In-Ceram/Vitadur Alpha porcelain laminates *International Journal of Prosthodontics* **13**(1) 66-71.
10. Fischer H, Schafer M, & Marx R (2003) Effect of surface roughness on flexural strength of veneer ceramics *Journal of Dental Research* **82**(12) 972-975.
11. Albakry M, Guazzato M, & Swain MV (2004) Effect of sandblasting, grinding, polishing and glazing on the flexural strength of two pressable all-ceramic dental materials *Journal of Dentistry* **32**(2) 91-99.
12. de Jager N, Feilzer AJ, & Davidson CL (2000) The influence of surface roughness on porcelain strength *Dental Materials* **16**(6) 381-388.
13. Quinn GD, Hoffman K, & Quinn JB (2012) Strength and fracture origins of a feldspathic porcelain *Dental Materials* **28**(5) 502-511.
14. Albakry M, Guazzato M, & Swain MV (2004) Influence of hot pressing on the microstructure and fracture toughness of two pressable dental glass-ceramics *Journal of Biomedical Materials Research Part B Applied Biomaterials* **71**(1) 99-107.
15. Scherrer SS, Kelly JR, Quinn GD, & Xu K (1999) Fracture toughness (K_{Ic}) of a dental porcelain determined by fractographic analysis *Dental Materials* **15**(5) 342-348.
16. Fredericci C, Yoshimura HN, Molisani AL, Pinto MM, & Cesar PF (2011) Effect of temperature and heating rate on the sintering of leucite-based dental porcelains *Ceramics International* **37**(3) 1073-1078.
17. Apetz R, & van Bruggen MPB (2003) Transparent alumina: A light-scattering model *Journal of the American Ceramic Society* **86**(3) 480-486.
18. Yoshimura HN, & Goldenstein H (2009) Light scattering in polycrystalline alumina with bi-dimensionally large surface grains *Journal of the European Ceramic Society* **29**(2) 293-303.
19. Prasad S, Monaco EA Jr, Kim H, Davis EL, & Brewer JD (2009) Comparison of porcelain surface and flexural strength obtained by microwave and conventional oven glazing *Journal of Prosthetic Dentistry* **101**(1) 20-28.
20. Sgura R, Reis MC, Hernandez AC, Fantini MCA, Andreetta MRB, & Medeiros IS (2013) Surface treatment of dental porcelain: CO₂ laser as an alternative to oven glaze *Lasers in Medical Science* <http://dx.doi.org/10.1007/s10103-013-1392-4>
21. Lawn BR, Evans AG, & Marshall DB (1980) Elastic-plastic indentation damage in ceramics—The median-radial crack system *Journal of the American Ceramic Society* **63**(9-10) 574-581.
22. Vichi A, Louca C, Corciolani G, & Ferrari M (2011) Color related to ceramic and zirconia restorations: A review *Dental Materials* **27**(1) 97-108.
23. Horcas I, Fernandez R, Gomez-Rodriguez JM, Colchero J, Gómez-Herrero J, & Baro AM (2007) WSXM: A software for scanning probe microscopy and a tool for nanotechnology *Review of Scientific Instruments* **78**(1) <http://dx.doi.org/10.1063/1.2432410>
24. Tholt de Vasconcellos B, Miranda-Junior WG, Prioli R, Thompson J, & Oda M (2006) Surface roughness in ceramics with different finishing techniques using atomic force microscope and profilometer *Operative Dentistry* **31**(4) 442-449.
25. Wee LM, Crouse PL, & Li L (2008) A statistical analysis of striation formation during laser cutting of ceramics *International Journal of Advanced Manufacturing Technology* **36**(7) 699-706.